Journal of Zhejiang University-SCIENCE B (Biomedicine & Biotechnology) 2022 23(1):58-73
www.jzus.zju.edu.cn; www.springer.com/journal/11585
E-mail: jzus_b@zju.edu.cn

Research Article

https://doi.org/10.1631/jzus.B2100155

Biocompatible chitosan/polyethylene glycol/multi-walled carbon nanotube composite scaffolds for neural tissue engineering

Shengbo SANG[1,2]✉, Rong CHENG[1,2], Yanyan CAO[1,2,3], Yayun YAN[1,2], Zhizhong SHEN[1,2,4], Yajing ZHAO[1,2], Yanqing HAN[5]

[1]*Shanxi Key Laboratory of Micro Nano Sensors & Artificial Intelligence Perception, College of Information and Computer, Taiyuan University of Technology, Taiyuan 030024, China*
[2]*Key Lab of Advanced Transducers and Intelligent Control System of the Ministry of Education, Taiyuan University of Technology, Taiyuan 030024, China*
[3]*College of Information Science and Engineering, Hebei North University, Zhangjiakou 075000, China*
[4]*Shanxi Six-Dimensional Artificial Intelligence Biomedical Research Institute, Taiyuan 030031, China*
[5]*Department of Neurology, Shanxi Provincial Cardiovascular Hospital, Taiyuan 030024, China*

Abstract: Carbon nanotube (CNT) composite materials are very attractive for use in neural tissue engineering and biosensor coatings. CNT scaffolds are excellent mimics of extracellular matrix due to their hydrophilicity, viscosity, and biocompatibility. CNTs can also impart conductivity to other insulating materials, improve mechanical stability, guide neuronal cell behavior, and trigger axon regeneration. The performance of chitosan (CS)/polyethylene glycol (PEG) composite scaffolds could be optimized by introducing multi-walled CNTs (MWCNTs). CS/PEG/CNT composite scaffolds with CNT content of 1%, 3%, and 5% (1%=0.01 g/mL) were prepared by freeze-drying. Their physical and chemical properties and biocompatibility were evaluated. Scanning electron microscopy (SEM) showed that the composite scaffolds had a highly connected porous structure. Transmission electron microscope (TEM) and Raman spectroscopy proved that the CNTs were well dispersed in the CS/PEG matrix and combined with the CS/PEG nanofiber bundles. MWCNTs enhanced the elastic modulus of the scaffold. The porosity of the scaffolds ranged from 83% to 96%. They reached a stable water swelling state within 24 h, and swelling decreased with increasing MWCNT concentration. The electrical conductivity and cell adhesion rate of the scaffolds increased with increasing MWCNT content. Immunofluorescence showed that rat pheochromocytoma (PC12) cells grown in the scaffolds had characteristics similar to nerve cells. We measured changes in the expression of nerve cell markers by quantitative real-time polymerase chain reaction (qRT-PCR), and found that PC12 cells cultured in the scaffolds expressed growth-associated protein 43 (GAP43), nerve growth factor receptor (NGFR), and class III β-tubulin (TUBB3) proteins. Preliminary research showed that the prepared CS/PEG/CNT scaffold has good biocompatibility and can be further applied to neural tissue engineering research.

Key words: Multi-walled carbon nanotube (MWCNT); Cell-scaffold; PC12 cells; Biocompatibility

1 Introduction

Neurological diseases are caused mainly by the death or loss of function of nerve cells. Because of the limitation of the location of damaged neurons in these diseases, only a small number of cells need to be replaced to achieve therapeutic purposes, so cell transplantation is expected to be an ideal treatment method (Abidian et al., 2012; Gu et al., 2014; Srinivasan et al., 2021). However, because of the limited supply of transplantable cells and their low viability after transplantation, the clinical application of this technology is greatly limited (Nisbet et al., 2008). With the development of tissue engineering technology, three-dimensional (3D) scaffolds with a porous structure can provide enough space for cells to grow, and facilitate the transmission of information and nutrients between cells, thus effectively promoting cell proliferation and differentiation (Runge et al., 2010; Mauro et al., 2013). A cell-scaffold is a network-like polymer capable of a high degree of water swelling that can effectively protect the activity of biomolecules (Uto et al., 2016). Its structure and mechanical properties are similar to

✉ Shengbo SANG, sunboa-sang@tyut.edu.cn
Shengbo SANG, https://orcid.org/0000-0003-3011-7632

Received Feb. 16, 2021; Revision accepted June 3, 2021;
Crosschecked Dec. 29, 2021

those of extracellular matrix (ECM), and it plays an important role in tissue engineering and drug delivery (Xu et al., 2016).

Nanomaterials can improve the physical properties of scaffolds, enhance their mechanical properties, and control their degradation and swelling rates. They can also affect the chemical structure of scaffolds and increase cell adhesion, proliferation, and differentiation. Nanomaterials are increasingly used in tissue engineering (Ahn et al., 2015). Şen and Culha (2016) reported the use of boron nitride nanotubes (BNNTs) and hydroxylated BNNT (BNNT-OH) to improve the performance of gelatin-glucose scaffolds prepared by electrospinning technology. Suner et al. (2019) prepared a cryogel composite with high mechanical strength and biocompatibility, based on various components of hyaluronic acid (HA) and halloysite nanotubes (HNTs), and revealed that an increased embedding of HNT into HA cryogels leads to an increase of mesenchymal stem cell (MSC) proliferation.

Carbon nanotube (CNT) is a nanomaterial currently undergoing rapid development (Park et al., 2011; Fabbro et al., 2013a). CNTs can enhance the inherent excellent properties of scaffolds: usually, once functionalized, they can improve mechanical stability, impart electrical conductivity, and serve as attachment sites for cells, macromolecules, or drug delivery carriers (Fabbro et al., 2013b; Bosi et al., 2014). They have also been used in other neural tissue engineering applications (Ghasemi-Mobarakeh et al., 2011; Liu et al., 2016; Rad et al., 2016). Importantly, although the biocompatibility of CNTs is still a concern, it has been shown that when CNTs are embedded in a scaffold matrix, their toxicity and carcinogenicity are greatly reduced (Posypanova et al., 2016; Zhou et al., 2018).

Various CNT composite scaffolds have been developed (Teo et al., 2016). They include some made from natural materials such as collagen and chitosan (CS), and some made from artificial synthetic materials such as polyethylene glycol (PEG) and polylactic acid (Wu et al., 2017; Bhaskar et al., 2018). The mechanical and biochemical properties of PEG are adjustable and can be strictly controlled. It also has a certain degree of hydrophilicity and good biocompatibility (Gao et al., 2016; Kotturi et al., 2017). Therefore, PEG can be used as a carrier for nerve cell delivery. (Runge et al., 2010; Ji et al., 2012; Shitole et al., 2019). In this study, we chose PEG as the nerve cell scaffold. The performance of a PEG scaffold can be improved after mixing with CS. CS is a natural cationic polysaccharide obtained by deacetylation of chitin (Duan et al., 2014; He et al., 2014). It is a biodegradable non-toxic polymer. For most tissues of the human body, CS has excellent biocompatibility and can effectively promote the proliferation and differentiation of nerve cells (Ifuku and Saimoto, 2012; Huang et al., 2014; Wu and Meredith, 2014). In addition, CS has obvious nerve conductivity and less nerve inducibility, enabling nerve cells to be induced to differentiate in the direction of neural networks (Jayakumar et al., 2011; Shokrgozar et al., 2011). Similarly, after adding CNTs to a CS/PEG scaffold, the strong interaction between hydrocarbon molecules can increase its porosity, surface roughness, and electrical conductivity, thereby increasing the adsorption efficiency of the scaffold (Mehdikhani and Ghaziof, 2018; Türk et al., 2018; van den Broeck et al., 2019).

In this study, CS/PEG/multi-walled CNT (MWCNT) composite scaffolds were prepared by a freeze-drying method, with CS/PEG and MWCNTs as the matrix. In addition, we studied the feasibility of applying MWCNTs to neural tissue engineering by adding different proportions of MWCNTs. The physicochemical properties of the composite scaffold were investigated. Furthermore, by culturing rat pheochromocytoma (PC12) cells in vitro, the cytotoxicity and cytocompatibility of the prepared composite scaffold were evaluated to assess its potential use in nerve regeneration (Wang et al., 2011; Posypanova et al., 2016; Zhou et al., 2018).

2 Materials and methods

2.1 Materials

MWCNTs ((20±3) nm in diameter and (3±2) μm in length) and PEG (molecular weight (MW)=6000) were purchased from Sigma Aldrich (Shanghai, China). CS (MW=85 000, >95% deacetylated) and epichlorohydrin (>99.5% purity) were purchased from Macklin Biochemical (Shanghai, China). The other chemicals, such as sodium hydroxide, acetic acid, and ethyl alcohol, were purchased from Sinopharm (Beijing, China). All other chemicals and reagents of analytical grade used were obtained without any further purification. Roswell Park Memorial Institute (RPMI)-1640, horse serum

(HS), fetal bovine serum (FBS), phosphate-buffered saline (PBS), and trypsin-ethylenediamine tetraacetic acid (EDTA) were purchased from Gibco (California, USA). PC12 cells, used for biocompatibility testing, were purchased from the Cell Bank of the Chinese Academy of Sciences (Shanghai, China).

2.2 Preparation of CS/PEG composite scaffolds

CS was dissolved in aqueous acetic acid (2%, volume fraction) at 60 °C to prepare a 0.02 g/mL CS solution, and then centrifuged to remove air bubbles. PEG was dissolved in 2% (volume fraction) acetic acid to obtain the 0.02 g/mL PEG solution. The PEG and CS solutions were thoroughly mixed at a volume ratio of 1:1 and stirred for 8 h to obtain the CS/PEG mixed solution, and 1.0 mol epichlorohydrin was added during the stirring process. The mixture was poured into a 24-well plate at room temperature to obtain a cross-linked CS/PEG scaffold.

2.3 Preparation of CS/PEG/CNT composite scaffolds

The preparation of composite materials with different concentrations of CNTs was as follows: a certain amount of purified CNTs was gradually dispersed into the above CS/PEG mixture by ultrasonic treatment for 30 min, and magnetically stirred for more than 8 h. The CNT concentrations were 1%, 3%, and 5% (1%=0.01 g/mL). Then, 1.0 mol epichlorohydrin was added to the mixture during stirring. The resulting CS/PEG/CNT composite was poured into a 24-well plate and placed in a −20 °C refrigerator to freeze for 12 h. Finally, the frozen mixture was freeze-dried by a freeze-dryer (Boyikang, Beijing, China) for 24 h.

2.4 Material characterization

2.4.1 SEM

The scaffolds were brittle-fractured and freeze-dried. Each cross-section was sputtered with gold, and then the microstructure of the scaffolds was observed by scanning electron microscopy (SEM; JEOL, Tokyo, Japan). The acceleration voltage was 5 V.

2.4.2 TEM

Transmission electron microscopy (TEM) images of ultrathin sections of lyophilized scaffolds were observed using a Hitachi Transmission Electron Microscope (HT7700, Hitachi, Japan) with an accelerating voltage of 200 kV. A copper grid coated with a holey carbon support film was used to prepare samples for TEM observation.

2.4.3 FT-IR spectroscopy

Freeze-dried scaffolds were tested with a Fourier transform infrared (FT-IR) spectrometer (Bruker ALPHA, Germany).

2.4.4 Raman spectroscopy

Raman of the lyophilized scaffolds was recorded with a Raman spectrometer (RM-1000, Renishaw, UK) with an Ar^+ laser and excitation at 532 nm ranging from 300 to 3200 cm^{-1}.

2.4.5 Mechanical properties

The uniaxial compression test (Norwood 5556 Research Institute, USA) was used to study the effect of the incorporation of CNTs on the Young's modulus of the scaffold. First, the initial diameter and thickness of each sample were measured, and the cross-sectional area of the scaffolds was calculated. Then a preload was slowly applied to the sample. The compression rate was set to 0.1 mm/min. After the scaffold was compressed to 50% of its original length, the Young's modulus was calculated based on the slope of the initial linear region of the stress-strain curve.

2.4.6 Water swelling

To evaluate the water swelling of the scaffolds, the freeze-dried scaffolds were first weighed, and then immersed in sterile PBS (0.1 mol/L, pH 7.4). After different specific time intervals, the scaffolds were removed from the PBS solution, and then immediately weighed after the surface was wiped with filter paper. The water swelling of the scaffolds at different time intervals was measured by gravimetric analysis, and calculated using the following formula:

$$\text{swelling} = (W_2 - W_1)/W_1 \times 100\%, \quad (1)$$

where W_1 and W_2 are dry weight and wet weight, respectively, of the scaffold.

2.4.7 Porosity

To measure the porosity of the scaffolds, the diameter and height of each freeze-dried scaffold were

measured to calculate its volume and then the scaffold was weighed. The scaffolds were then immersed in ethanol, and placed in a vacuum-drying oven at reduced pressure to remove bubbles. Finally the sample was weighed immediately after the surface was wiped with filter paper. Porosity (P) was calculated by the following formula:

$$P=(W_4-W_3)/V_1\times qe\times 100\%, \tag{2}$$

where W_3 is the initial dry weight of the scaffolds, W_4 is the weight after immersion in ethanol under reduced pressure to remove bubbles, V_1 is the volume of the initial freeze-dried scaffold, and qe refers to the ethanol density of 0.789 mg/mL.

2.4.8 Conductivity

Before performing the conductivity study, the different scaffolds were immersed in pure deionized water for 3 d, with the water being replaced at least five times. Then the scaffolds were cut into rectangular pieces and the length, width, and height of cuboids were measured. A Fluke 73 multimeter (VICTOR, Shenzhen, China) was used to measure the resistance of these scaffolds. The resistivity (ρ) was calculated according to the following formula:

$$\rho=RA/L=RWH/L, \tag{3}$$

where A is the cross-sectional area of the cuboid; L, W, and H are the length, width, and height, respectively, of the initial freeze-dried scaffold; and R represents the resistance of the scaffold.

2.4.9 In vitro biodegradation

To study the in vitro degradability of the scaffolds, the CS/PEG/CNT scaffolds were hydrolyzed in PBS (pH=7.4, 37 ℃) and PBS with lysozyme (4 mg/mL, pH=7.4, 37 ℃) in vitro enzymolysis. The lyophilized scaffolds were weighed, and then immersed in the above two solutions. The solutions were changed once a week. The scaffolds were removed from the solution at specific time intervals and washed thoroughly with deionized water. They were then freeze-dried and weighed. According to the percentage of the residual weight of the dried scaffold before and after the PBS or lysozyme treatment, which represents the remaining weight of the scaffold, the degree of in vitro biodegradation was calculated by the following formula:

$$\text{weight remaining}=W_5/W_3\times 100\%, \tag{4}$$

where W_5 is the dry weight after several days of treatment with lysozyme (or PBS).

2.5 Proliferation and spreading

Neuronal PC12 cells can be used for cytotoxicity and cytocompatibility studies. PC12 cells were cultured at 37 ℃ in 5% (volume fraction) CO_2 in RPMI-1640 with 10% (volume fraction) HS, 5% (volume fraction) FBS, and 1% (volume fraction) penicillin-streptomycin. 3-(4.5-Dimethylthiazol-2-yl)-2,5-diphenyltetrazolim bromide (MTT) was used to evaluate the proliferation of cells on different scaffolds. The sterilized scaffolds were placed into a 96-well plate, and 200 μL PC12 cell suspension was seeded onto the scaffolds at 5×10^4 cells/mL. The fresh medium was changed every 2 d. After 1, 3, 5, and 7 d of incubation, 20 μL MTT (5 mg/mL, prepared with PBS, pH=7.4) was added to each well and incubated for 4 h. The culture was then terminated and the supernatant was aspirated. Dimethyl sulfoxide (DMSO, 200 μL) was added to each hole. After incubation on a shaker for 10 min, 150 μL supernatant was placed into a new 96-well microplate and the optical density (OD) at 570 nm was measured.

To evaluate the adhesion rate of PC12 cells on the scaffold, sterilized scaffolds (0.5 cm×0.5 cm×0.5 cm) were placed in a 96-well plate with culture medium and cultured for 12 h. Then 0.1 mL of PC12 cell suspension was seeded on each scaffold (seeding density (C) $=1\times10^5$ cells/mL). After 4 h of culture, scaffolds were removed and the number of remaining cells was recorded as N_R. The cell adhesion rate was calculated using the following formula:

$$\text{adhesion rate}=(CV-N_R)/CV\times 100\%, \tag{5}$$

where V is the volume of scaffold.

2.6 Live/dead assay

To study the toxicity of the scaffolds, a live/dead cell staining experiment was performed. Live and dead cells were stained by calcein acetoxymethyl ester (calcein-AM)/propidium iodide (PI) (BestBio, Shanghai,

China). After the PC12 cells were seeded on the scaffolds (30 000 cells/cm^2) and cultured for 3 d, the medium was removed and the scaffolds were washed with PBS for staining. The morphology of the stained cells was photographed using a Cytation5 Imaging Reader (BioTek, USA). The numbers of live and dead cells and the average cell size were analyzed from the fluorescence images.

2.7 Neuron differentiation

To evaluate the development of neurites, PC12 cells were seeded on scaffolds (30 000 cells/cm^2), and 50 ng/mL nerve growth factor (NGF) was added to the culture medium to induce cell differentiation. After 4 d, the medium was aspirated and the scaffolds were washed with PBS. The scaffolds were then fixed with 4% (volume fraction) paraformaldehyde (PFA) solution and infiltrated with 0.3% (volume fraction) Triton X-100 solution. Phalloidin was used to stain the cytoskeleton attached to the scaffold, and fluorescence images were read using the Cytation5 Imaging Reader.

2.8 Immunofluorescence

After 4 d of differentiation culture, the cell-scaffolds were taken out and washed with PBS. Then they were fixed with pre-cooled 4% PFA for 30 min, followed by infiltration with 0.3% Triton X-100 solution for 20 min. After that, the scaffolds were blocked with 2% (volume fraction) goat serum blocking solution for 1 h, and incubated with antibody diluent growth-associated protein 43 (GAP43), which was diluted with 2% (volume fraction) bull serum albumin (BSA) at 1:200 (volume ratio, the same below), at 4 ℃ overnight. The next day, the cell-scaffolds were reacted with the secondary antibody diluent Cy3-rbit (diluted with 2% BSA at 1:500) for 30 min and incubated with diamidine phenyl indole (DAPI) solution for 15 min at room temperature. Fluorescent images were captured using the Cytation5 Imaging Reader.

2.9 Quantitative RT-PCR

Total RNA was extracted from scaffold-free cell cultures using TRIzol reagent (Sigma, Shanghai, China), as a positive control. Similarly, after 4 d of differentiation culture, total RNA was extracted from the cells on the scaffolds. The white RNA pellet obtained was dissolved in RNase-free water, and the RNA concentration was measured with a spectrophotometer (Thermo Scientific, Shanghai, China). The total complementary DNA (cDNA) was synthesized with a cDNA synthesis kit (Juhemei, Beijing, China). SYBR Premix Ex Taq (Juhemei, Beijing, China) was used for quantitative real-time polymerase chain reaction (qRT-PCR). Table 1 shows the gene-specific primers used for *GAP43*, NGF receptor (*NGFR*), and class III β-tubulin (*TUBB3*). The CFX96^{TM} RT-PCR detection system (BioRad, USA) was used to quantify the SybrGreen fluorescence of the amplified cDNA products. Each sample and positive control were analyzed by three qRT-PCR reactions. The results of qRT-PCR analysis are expressed as the average amount of expression of each gene relative to that of the reference gene (glyceraldehyde-3-phosphate dehydrogenase (*GAPDH*)).

Table 1 Sequences of the qRT-PCR primers

Gene	Primer sequence
GAP43	
Sense	5'-TGAGGAGAAGAAGGGCGAAGGG-3'
Antisense	5'-AGGACGGCGAGTTATCAGTGGTAG-3'
NGFR	
Sense	5'-CCTGCTGCTGCTGCTGATTCTAG-3'
Antisense	5'-CCACGCCTTCGCCCAAGTTG-3'
TUBB3	
Sense	5'-CGTCCACCTTCATCGGCAACAG-3'
Antisense	5'-TCGGCCTCGGTGAACTCCATC-3'

qRT-PCR: quantitative real-time polymerase chain reaction; *GAP43*: growth-associated protein 43; *NGFR*: nerve growth factor receptor; *TUBB3*: class III β-tubulin.

2.10 Statistical analysis

All of the numerical data were statistically analyzed using SPSS software (Version 17.0, International Business Machine, Beijing, China). The data are expressed as mean±standard deviation (SD). Statistical analysis included a one-way analysis of variance (ANOVA). Differences were considered statistically significant when $P<0.05$.

3 Results and discussion

3.1 Morphological characteristics of CS/PEG/CNT scaffold

Fig. 1a shows the process for preparation of the composite scaffold. Fig. 1b shows a schematic diagram of the possible interaction between CS/PEG nanofibers

and CNT nanofibers in the process of forming a CS/PEG/CNT composite scaffold. The hydrophilic amino groups, hydroxyl groups, and the extremely hydrophobic methyl groups of CNTs on CS undergo intermolecular interactions through static electricity. During the regeneration process, because of the close combination of CS/PEG and CNT nanofiber bundles, a dense porous structure is formed, which can effectively improve the mechanical properties of the scaffold.

To understand the structural changes caused by CNTs, we imaged CS/PEG scaffolds without CNTs and with different concentrations of CNTs under SEM (Figs. 2a–2h). We observed that the CS/PEG scaffold exhibited a porous network structure (Fig. 2a). This is because the solvent and non-solvent CS and PEG solutions are exchanged by diffusion, and the nanofiber bundles are formed by parallel self-aggregation (Lau et al., 2008; Türk et al., 2018). The pore size of the CNT-containing scaffold was relatively small, and because of the presence of CNTs, some pore-like structures also appeared on the pore wall of the scaffold, an area more conducive to cell adhesion (Figs. 2e–2h). To study the dispersibility of CNTs in the CS/PEG matrix, ultra-thin cross-sections of CS/PEG and CS/PEG/CNT freeze-dried scaffolds were further examined by TEM. CNTs are long strips with a diameter of 20–30 nm. As shown in Figs. 2i–2l, CNTs were well dispersed in the CS/PEG matrix and combined with the CS/PEG nanofiber bundles.

3.2 Molecular structure of CS/PEG/CNT scaffold

Fig. 3a shows the FT-IR spectra of the different types of scaffolds. Two peaks around 3450 and 962 cm^{-1} in the spectra of CS/PEG/CNT and CS/PEG scaffolds were assigned to terminal hydroxyl (OH) and polyether C–O stretching. After adding CNTs, the peak at 3450 cm^{-1} may have been due to the presence of oxygen-containing groups such as OH and carboxylic acid (COOH), which stretched the bound OH. In the spectra of the CS/PEG/CNT blend composite and CS/PEG scaffolds, the tensile vibration peaks at 2988 and 1109 cm^{-1} are indicated for C–H alkane stretching and for C–O–C as a result of the formation of a cross-linked network structure, respectively. In addition, there are characteristic CS peaks around the amino and amide groups at 1466 and 1636 cm^{-1}.

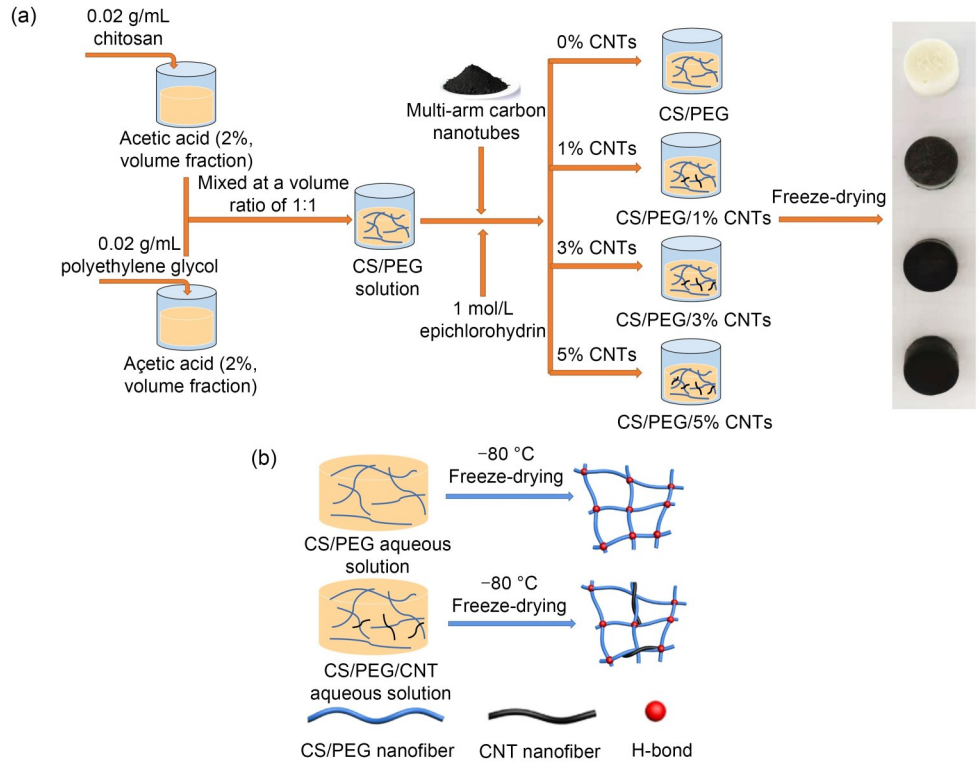

Fig. 1 Process for preparation of the composite scaffold (a) and schematic representation of the construction of CS/PEG and CS/PEG/CNT scaffolds (b). For CNT concentration, 1%=0.01 g/mL. CS: chitosan; PEG: polyethylene glycol; CNT: carbon nanotube.

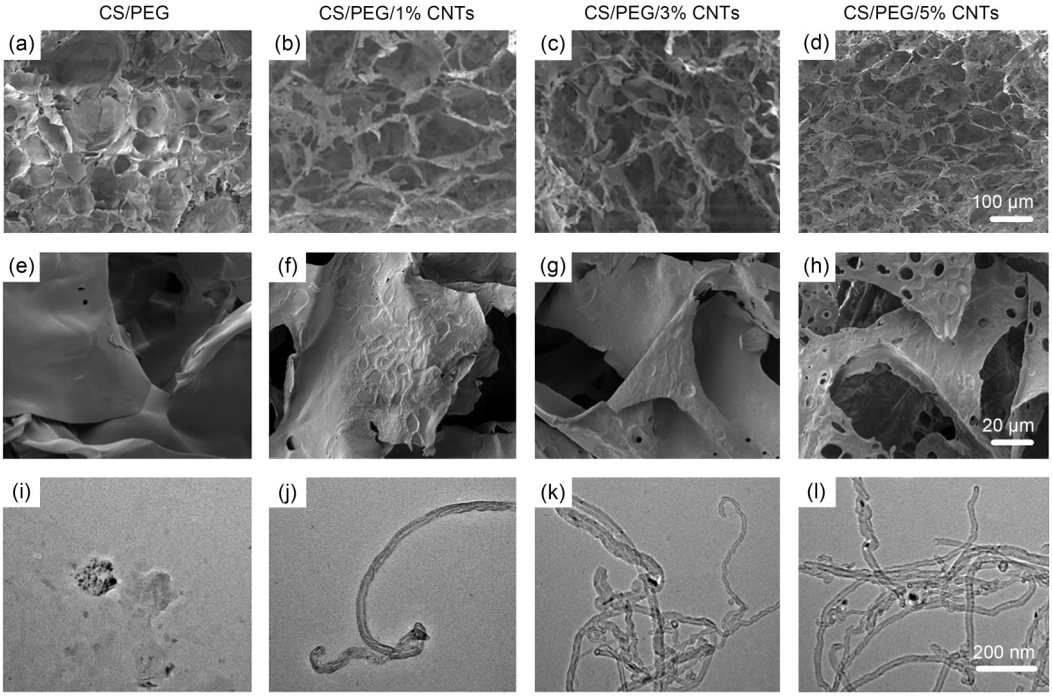

Fig. 2 SEM images (a–h) and TEM images (i–l) of the surfaces of the lyophilized scaffolds. (a, e, i) CS/PEG; (b, f, j) CS/PEG/1% CNTs; (c, g, k) CS/PEG/3% CNTs; (d, h, l) CS/PEG/5% CNTs. For CNT concentration, 1%=0.01 g/mL. SEM: scanning electron microscopy; TEM: transmission electron microscopy; CS: chitosan; PEG: polyethylene glycol; CNT: carbon nanotube.

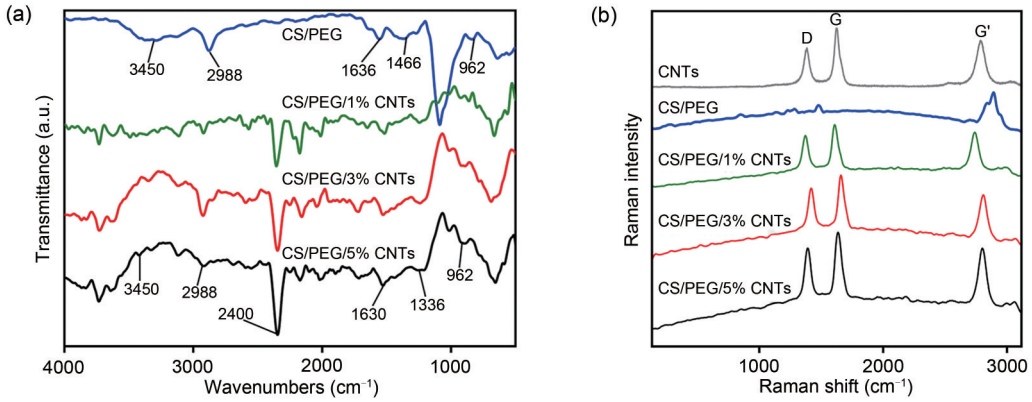

Fig. 3 FT-IR spectra (a) and Raman spectroscopy (b) of CS/PEG, CS/PEG/1% CNT, CS/PEG/3% CNT, and CS/PEG/5% CNT composite scaffolds. For CNT concentration, 1%=0.01 g/mL. FT-IR: Fourier transform infrared; CS: chitosan; PEG: polyethylene glycol; CNT: carbon nanotube; a.u.: arbitrary unit.

CNTs have a unique Raman spectrum with three characteristic bands: the D band and defect peaks of amorphous carbon appear between 1250 and 1450 cm^{-1}, and the G band comes from the planar tangential stretching of CNTs. The C–C bond in the graphene sheet appears at 1584–1590 cm^{-1}, and the G' band of the second-order overtone of the D band appears at 2705–2715 cm^{-1}. Raman spectroscopy can be used to prove the presence of CNTs in composite samples. As shown in Fig. 3b, the main characteristics of CNTs were observed in the Raman spectrum of the freeze-dried CS/PEG/CNT scaffold, and the intensity of the characteristic peaks increased with increasing CNT concentration, indicating the presence of CNTs.

The Young's modulus of the scaffold is shown in Fig. 4a. Composite materials used for cell culture and

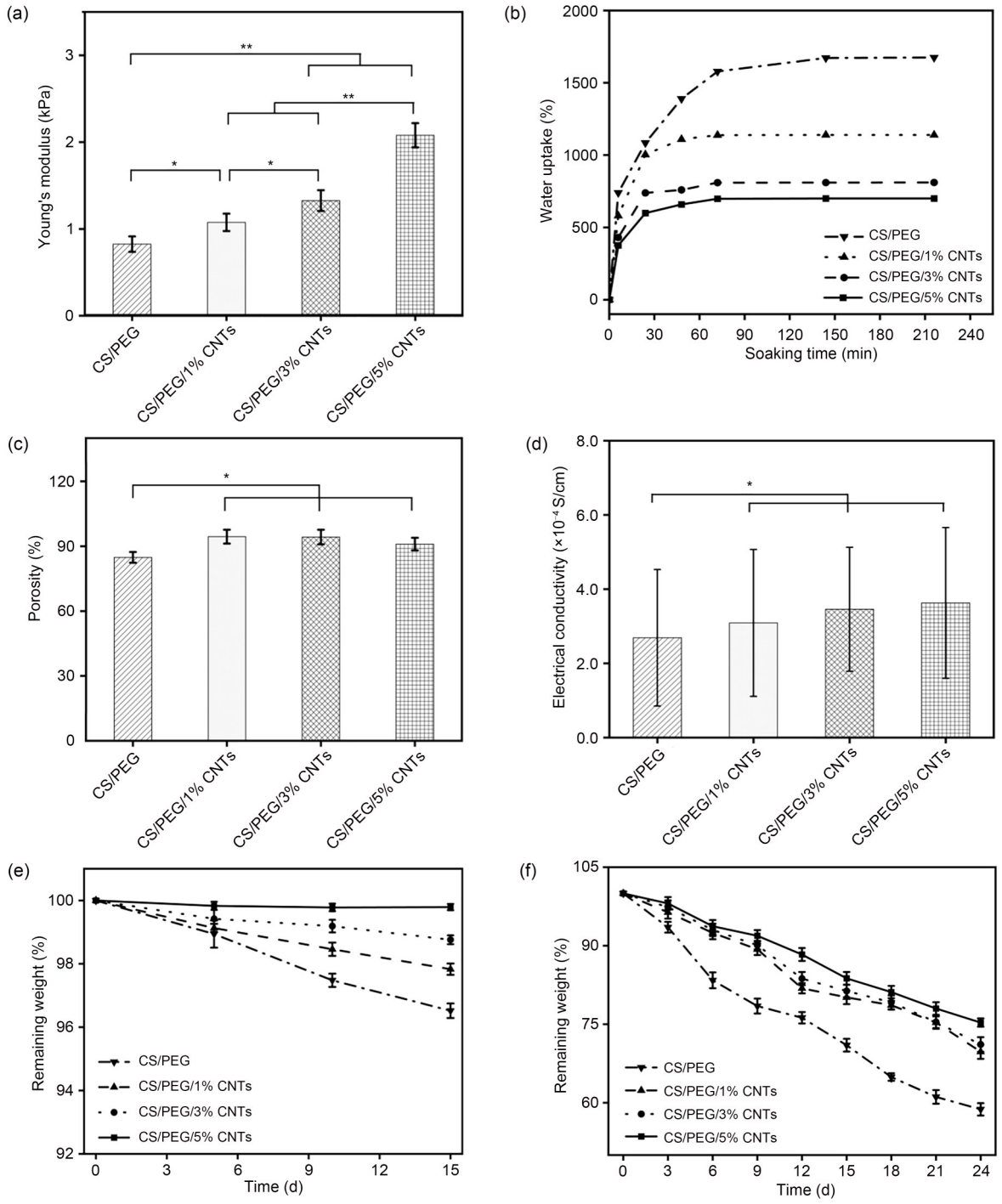

Fig. 4 Characterization of the lyophilized CS/PEG, CS/PEG/1% CNT, CS/PEG/3% CNT, and CS/PEG/5% CNT composite scaffolds. (a) Young's modulus; (b) Swelling rate; (c) Porosity; (d) Conductivity; (e, f) In vitro biodegradation in PBS (e) and 4 mg/mL lysozyme (f) at pH 7.4 and 37 °C. For CNT concentration, 1%=0.01 g/mL. Data, except those in (b), are expressed as mean±standard deviation (SD), n=3. $^{*}P$<0.05, $^{**}P$<0.01. CS: chitosan; PEG: polyethylene glycol; CNT: carbon nanotube; PBS: phosphate-buffered saline.

biomedical implantation should be able to withstand high loads. So understanding the mechanical properties of composite materials is essential for the application of cell scaffolds (Nagarajan et al., 2017). The Young's modulus of the CS/PEG scaffold was 0.79 kPa. In contrast, after adding CNTs, the mechanical properties

of CS/PEG/CNT scaffolds showed obvious enhancement and toughening effects. When the concentrations of CNTs added were 1%, 3%, and 5%, the Young's modulus values were 1.17, 1.32, and 2.09 kPa, respectively. This is due to the high physical crosslink density of scaffolds after addition of CNTs. In general, scaffolds with added CNTs exhibited good mechanical properties, and as the concentration of CNTs increased, the Young's modulus of the scaffolds continued to increase.

At various time intervals, the water swelling of CS/PEG and CS/PEG/CNT scaffolds with different concentrations of CNTs was measured (Fig. 4b). All these scaffolds showed a rapid increase in water swelling and reached a state of high swelling equilibrium at around 60 min. After adding CNTs, the degree of swelling of the scaffold was reduced further (Fig. 4b). This may have been because mixing the CS/PEG scaffold with CNTs reduced the physical bond between OH and NH_2 groups, so there were more water binding points. CNTs can be mixed with CS/PEG scaffolds to improve their adsorption to cells by increasing their binding sites.

Fig. 4c shows that the porosity of the scaffolds varied from 85% to 95%. The differences among the scaffolds were increased significantly after adding CNTs (P<0.05), but the concentration of CNT had little effect on the porosity of the scaffold. This indicated that the addition of CNTs did not significantly affect the porosity of the composite scaffold. Porosity is very important for cell growth and migration, waste transportation, and nutrient acquisition. Generally, the higher the porosity, the more space and nutrients for cells and tissues. Based on the above hypothesis and experimental results, the CS/PEG/CNT scaffold with higher porosity in this study may be beneficial to the regeneration of peripheral nerves (Türk et al., 2018).

In nerve tissue engineering, cell scaffolds need to promote the growth and development of neurites and promote nerve regeneration, so nerve cell scaffolds need to have a certain degree of conductivity. Generally, the commonly used physiological stimulus value is 100 mV, and the biologically effective current ranges from 0.6 to 400 μA. When the conductivity of a scaffold is higher than 1.0×10^{-4} S/cm, it can be used for nerve tissue regeneration (Ma et al., 2014). In this study, we found that after adding conductive materials (CNTs), the conductivity of the porous composite scaffold was significantly improved (P<0.05). In other words, the composite scaffolds of CS/PEG ($(2.69\pm1.84)\times10^{-4}$ S/cm), CS/PEG/1% CNT ($(3.09\pm1.98)\times10^{-4}$ S/cm), CS/PEG/3% CNT ($(3.46\pm1.67)\times10^{-4}$ S/cm), and CS/PEG/5% CNT ($(3.63\pm2.03)\times10^{-4}$ S/cm) can be used as conductive substrates suitable for electrical stimulation research. With the increase of CNT content, the conductivity of the composite scaffold showed an increasing trend, reaching up to 134.94% of the control group (Fig. 4d). This may be because of the increased content of CNTs, which increases the tube-to-tube contact. Also, π electrons can move between the tubes at high speed, thereby increasing the conductivity of the scaffold (Mattioli-Belmonte et al., 2012).

As the incubation time increased, the residual weight of the scaffolds decreased slightly and maintained a higher plateau at the end (Fig. 4e). Compared with the CS/PEG scaffold, the stability of the CS/PEG/CNT composite scaffold to PBS increased with increasing CNT concentration, which is conducive to the feasible storage and transportation of the scaffold. In contrast to the degradation in PBS, during the test, the remaining weight of the scaffold was observed to decrease almost linearly with enzymatic hydrolysis (Fig. 4f). The CS/PEG scaffold degraded 17.7% in 3 d and 42.8% in 24 d after immersion in the lysozyme solution. The degradation products were reported to be non-toxic glucosamine and *N*-acetyl glucosamine (Venkatesan et al., 2012). Because of the interaction between CS/PEG and CNTs and the formation of a more uniform and dense microstructure after adding CNTs, its degradation rate was relatively slow. After 24 d in the lysozyme solution, the biodegradation rate of the CS/PEG/5% CNT scaffold was about 24.6% (75.4% of the highest residual rate), but this was lower than that of the CS/PEG scaffold. Therefore, the CS/PEG/CNT scaffold has a feasible biodegradation rate when it contains lysozyme, and the soluble CNTs released in this process can be excreted in urine. All the above factors can help the tissue scaffold maintain its shape and mechanical properties in the early stages of organ regeneration and biodegradation, so that it is more effective for nerve regeneration and repair, and can be used in clinical trials.

3.3 Proliferation of PC12 cells on scaffolds

To study the biocompatibility and potential regulation of neuronal cells when CS/PEG/CNT scaffolds

are used as substrates for neuronal growth, MTT analysis was used following co-culture for 1, 3, 5, and 7 d. Fig. 5a shows the effect of the scaffold on the proliferation ability of PC12 cells. The PC12 cells on the scaffold showed greater proliferation ability than those cultured without the scaffold. As the culture time increased and the concentration of CNTs in the CS/PEG matrix increased, the cell viability also increased, indicating that the scaffold has no cytotoxicity and can promote the proliferation of neuronal cells. When the concentration of CNTs was higher, the cell growth decreased slightly, which may have been due to mechanical damage caused by the scaffold when it was adsorbed to the cell wall or membrane (Naumenko and Fakhrullin, 2019). Therefore, the CS/PEG/CNT scaffold has good biocompatibility and can be used as a matrix for guiding the growth of nerve ducts during neuron repair. When the CNTs content was 3%, the cells on the scaffold had higher cell viability. This may have been because the added CNTs could absorb the nutrients in the medium and make them adhere to the scaffold, and the surrounding enrichment was beneficial for cell growth.

The effect of scaffolds on cell adhesion was also investigated. Generally speaking, because of the hydrophilicity of the cell membrane, the hydrophilic surface of the material will be conducive to cell adhesion. However, because cell adhesion requires protein-mediation, the scaffold must have a certain hydrophobicity (Eldesoqi et al., 2014). As the concentration of CNTs increased, the cell adhesion rate also increased (Fig. 5b). This may have been because CNTs can reduce the hydrophilicity of a scaffold. The cell adhesion rate was also related to the porosity and surface roughness of the scaffold. The greater the porosity, the greater the contact area between the cells and the scaffold. A rough surface could enhance the adsorption capacity of the scaffold to the culture medium, thereby promoting cell adhesion. These results in Fig. 5 indicated that adding CNTs to the CS/PEG cell scaffold has a positive effect on cell adhesion and proliferation. PEG has the unique property of inhibiting non-specific protein adsorption. When PEG is combined with crystalline polymers, nanoparticles or microparticles, and nano or ultrafine fibers, it will further enhance the cell behavior of a variety of cell types. In this study, compared with PEG/CS scaffolds, the addition of CNTs can make conductive scaffolds have many advantages, such as improving cell attachment and proliferation capabilities.

3.4 Cytotoxicity of composite scaffolds

The cytotoxicity of these scaffolds on PC12 cells was evaluated by live/dead cell analysis. Calcein-AM can make living cells fluoresce green, while PI can make dead cells fluoresce red. As the CNT concentration increased, more green fluorescent cells were seen on the scaffold (Figs. 6a–6d). Quantitative analysis of the number of live/dead cells on these scaffolds showed that the CS/PEG/3% CNT scaffold had the highest number of PC12 cells (Fig. 6e), and all scaffolds had almost no cytotoxicity. Cells on the CS/PEG/3% CNT

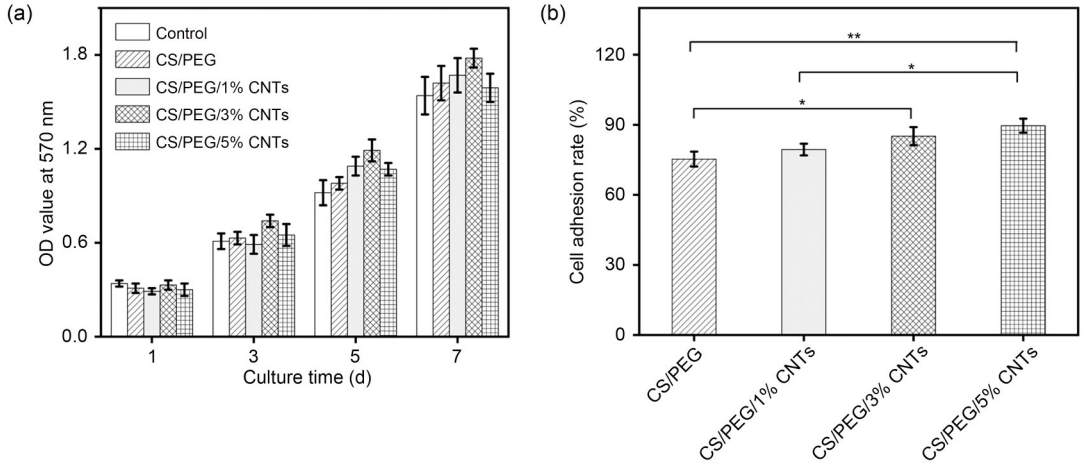

Fig. 5 Cell proliferation (a) and adhesion (b) on scaffolds with different CNT concentrations. For CNT concentration, 1%=0.01 g/mL. Data are expressed as mean±standard deviation (SD), n=3. * P<0.05, ** P<0.01. OD: optical density; CS: chitosan; PEG: polyethylene glycol; CNT: carbon nanotube.

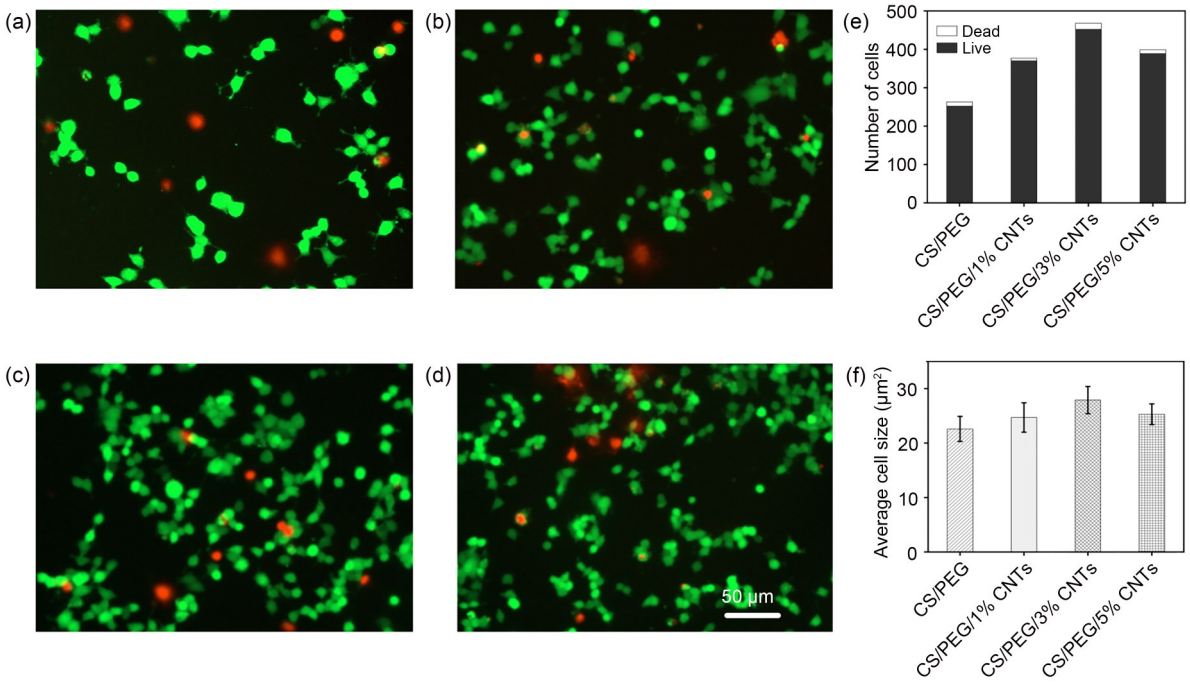

Fig. 6 PC12 cell survival on CS/PEG (a), CS/PEG/1% CNT (b), CS/PEG/3% CNT (c), and CS/PEG/5% CNT (d) scaffolds, the number of living and dead cells (e), and the average size of cells calculated from fluorescence images of the cells on the different scaffolds (f). Cell survivability analysis: live (green) and dead (red). For CNT concentration, 1%=0.01 g/mL. Data are expressed as mean±standard deviation (SD), *n*=3. CS: chitosan; PEG: polyethylene glycol; CNT: carbon nanotube (Note: for interpretation of the references to color in this figure legend, the reader is referred to the web version of this article).

scaffold were the largest and most differentiated (Fig. 6f). Compared with the CS/PEG scaffold, after adding CNT, PC12 cells maintained higher cell viability and better cell morphology. It is worth noting that after 3 d of incubation, the diffusion area of PC12 cells on CS/PEG/CNTs was (27.9±2.5) μm^2, while the diffusion area of PC12 cells on CS/PEG scaffold was (22.6±2.3) μm^2. In summary, the good biocompatibility of the CS/PEG/3% CNT composite scaffold makes it a promising material for tissue engineering applications.

3.5 Neuronal differentiation of PC12 cells on scaffolds

After 50 ng/mL NGF was used to induce differentiation, PC12 cells on these scaffolds were stained with phalloidin (Figs. 7a–7d), and the length of neurites formed from each cell was determined. The neurites in the cells on the CS/PEG scaffold were all aggregated within 50 μm, with an average value of (11.9±9.1) μm. For scaffolds with CNT content of 1% and 5%, some neurites had average lengths of (14.6±10.3) and (16.2±12.3) μm, respectively. Some neurites formed by the cells on the CS/PEG/3% CNT scaffold were more than 50 μm long, with an average value of (17.3±13.9) μm (Fig. 7e). The circularity of each nucleus was calculated, and then the reciprocal of the nuclear circularity was used to obtain the elongation of the nucleus. The results showed that when the CNT content was 3%, the nuclei of the cells on the scaffold were more stretched (Fig. 7f). These results may indicate that CNT can promote the differentiation of neurons and provide an ideal effect for the cultivation of the nervous system. With these advantages, the 3D conductive scaffold structure is expected to become an efficient nerve culture system for nerve tissue engineering.

3.6 Protein expression of PC12 cells on scaffolds

The immunofluorescence experiment confirmed the ability of the different scaffolds to promote differentiation. After seeding the cells on the scaffold, NGF was used to induce the differentiation of PC12 cells for 4 d, and the GAP43 was used to test their degree of differentiation. A second antibody labeled with green fluorescence was used to identify the protein, and the

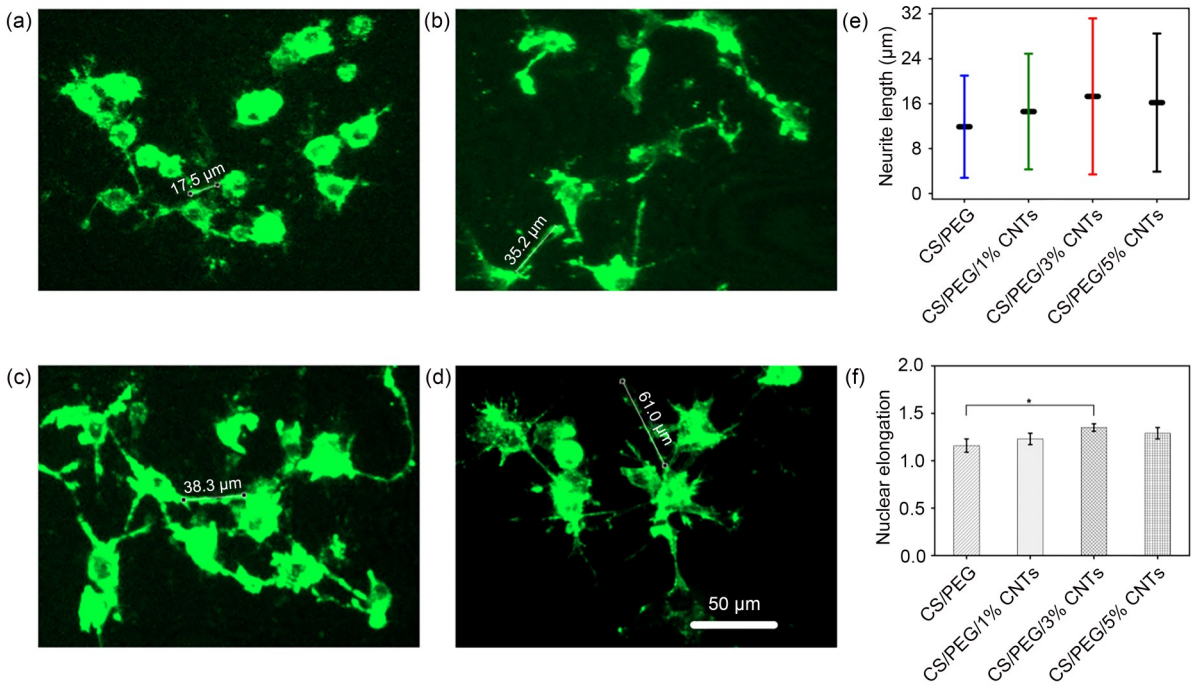

Fig. 7 Differentiation of PC12 cells induced by CS/PEG (a), CS/PEG/1% CNT (b), CS/PEG/3% CNT (c), and CS/PEG/5% CNT (d) scaffolds revealed by phalloidin staining, the distribution and average values of the length of neurites formed in the cells grown (e) and the elongation of nuclei (f) on the scaffolds. For CNT concentration, 1%=0.01 g/mL. Data are expressed as mean±standard deviation (SD), n=3. * P<0.05. CS: chitosan; PEG: polyethylene glycol; CNT: carbon nanotube.

nucleus was stained with DAPI to determine the location of the nucleus. The stronger the green fluorescent signal, the higher the degree of differentiation. As shown in Fig. 8, with increasing CNT concentration, the effect of the scaffold on the promotion of differentiation of PC12 cells continued to increase. The ability of the PC12 cells to differentiate was strongest when the CNT concentration was 3%, indicating that the CNT scaffold can promote the differentiation of PC12 cells. These results may indicate that because CNTs enhance the roughness of the scaffold, leading to increased neuronal differentiation, the conductive scaffold structure provides the desired effect. With these advantages, the 3D conductive scaffold structure is expected to become an efficient nerve culture system for nerve tissue engineering.

3.7 Gene expression of PC12 cells on scaffolds

After 4 d of inoculation of PC12 cells on the scaffold, the expression levels of markers (*GAP43*, *TUBB3*, and *NGFR*) related to PC12 cell differentiation in the extracted total RNA were detected by fluorescent qRT-PCR. GAP43 is a nerve-specific protein that is related to neurite outgrowth, so it can be used as a marker for differentiation of PC12 cells. NGFR is a nerve growth factor receptor. TUBB3 is a neuronal cell-specific tubulin (Stock et al., 2010). The expression level of *GAP43* was significantly lower than those of *TUBB3* and *NGFR* (Fig. 9), and remained at a very low level throughout the differentiation process. In the same group, as the concentration of CNTs increased, the expression levels of different genes also increased. The expression levels of *GAP43* on different scaffolds were not significantly different (Fig. 9a). The expression levels of *NGFR* and *TUBB3* in the cells on the scaffolds were significantly higher than in those without the scaffolds (Figs. 9b and 9c; P<0.01). When CNTs were added to the scaffold, the expression levels of *NGFR* and *TUBB3* in the cells on the scaffold were also significantly increased (Figs. 9b and 9c; P<0.05). In general, the expression of markers related to PC12 cell differentiation was highest when the concentration of CNTs was 3%.

4 Conclusions

In this study, a CS/PEG scaffold was first prepared, and MWCNTs of different concentrations

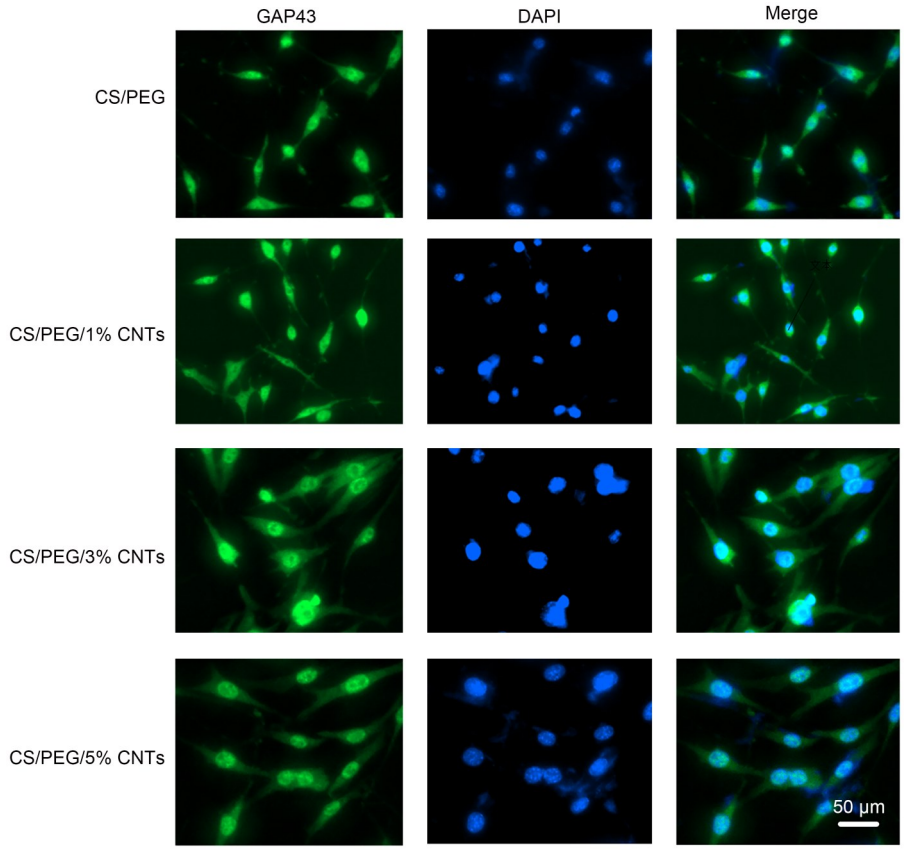

Fig. 8 Immunofluorescent identification of cells inoculated on CS/PEG, CS/PEG/1% CNT, CS/PEG/3% CNT, and CS/PEG/5% CNT scaffolds for 4 d, and the expression of GAP43 protein. For CNT concentration, 1%=0.01 g/mL. CS: chitosan; PEG: polyethylene glycol; CNT: carbon nanotube; GAP43: growth-associated protein 43; DAPI: diamidine phenyl indole.

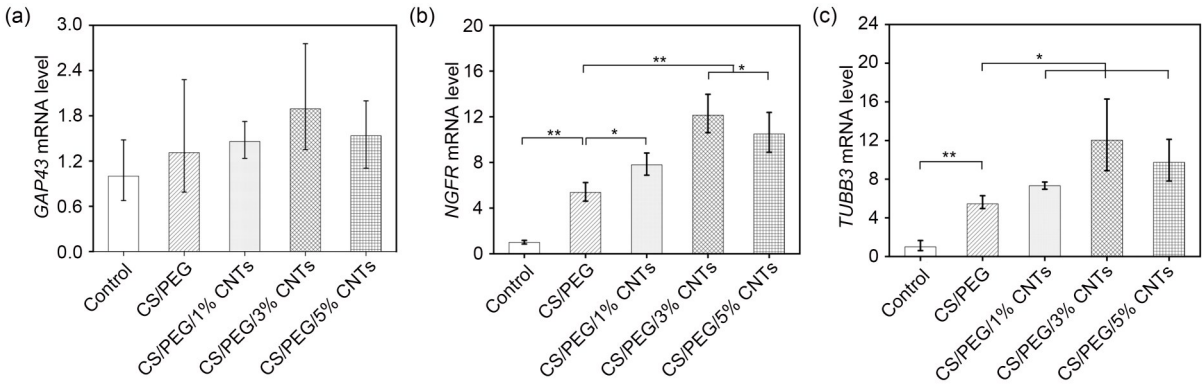

Fig. 9 qRT-PCR results showing the mRNA levels of *GAP43* (a), *NGFR* (b), and *TUBB3* (c) on different scaffolds and in untreated cells. *GAPDH* was used as an internal reference, and the experimental data are expressed as mean±standard deviation (SD), n=3. $^{*}P$<0.05, $^{**}P$<0.01. For CNT concentration, 1%=0.01 g/mL. CS: chitosan; PEG: polyethylene glycol; CNT: carbon nanotube; *GAP43*: growth-associated protein 43; *NGFR*: nerve growth factor receptor; *TUBB3*: class III β-tubulin; *GAPDH*: glyceraldehyde-3-phosphate dehydrogenase; qRT-PCR: quantitative real-time polymerase chain reaction.

were successfully dispersed in the CS/PEG scaffold by ultrasonic treatment to prepare CS/PEG/CNT scaffolds. In this process, epichlorohydrin was used as the crosslinking agent. SEM images showed that the CS/PEG/CNT scaffolds exhibited a tight and neat hollow network structure. Raman spectroscopy showed

the presence of CNTs in the composite scaffold, and TEM further proved that CNTs were well dispersed in the CS/PEG matrix. The addition of CNTs increased the roughness, conductivity, and hydrophobicity of the pore wall of the scaffolds. The scaffold porosity was 83%–96%, which meets the requirements for cell growth. The mechanical properties of the scaffolds were enhanced by the addition of CNTs, and the swelling rate and biodegradation rate were reduced. The results of in vitro biological evaluation of PC12 cells showed that the CS/PEG/CNT scaffold had good biocompatibility without cytotoxicity, and enhanced neuronal cell proliferation and differentiation ability in vitro. As an increase of CNTs increased the roughness of the scaffold, the PC12 cells cultured on the CS/PEG/CNT scaffold showed great neurite extension. As the concentration of CNTs increased, this trend became more obvious. To evaluate the possibility of PC12 cells differentiating into nerve cells, we analyzed the expression patterns of the nerve cell-specific markers *GAP43*, *NGFR*, and *TUBB3*. The expression of nerve cell markers was confirmed by immunofluorescence staining and qRT-PCR. In general, the CS/PEG/CNT scaffold has excellent and comprehensive properties, and is expected to be used as a neuron growth substrate for peripheral nerve regeneration.

Acknowledgments

This study was supported by the National Natural Science Foundation of China (Nos. 51975400 and 62031022) and the Shanxi Provincial Key Medical Scientific Research Project (No. 2020XM06), China.

Author contributions

Shengbo SANG and Rong CHENG designed the research, wrote the manuscript, and are primarily responsible for final content. Yanyan CAO and Yayun YAN conducted a characterization experiment of the scaffold and revised the manuscript. Zhizhong SHEN conducted cell culture. Yajing ZHAO and Yanqing HAN conducted cell experiments and explained them. All authors have read and approved the final manuscript, and therefore, have full access to all the data in the study and take responsibility for the integrity and security of the data.

Compliance with ethics guidelines

Shengbo SANG, Rong CHENG, Yanyan CAO, Yayun YAN, Zhizhong SHEN, Yajing ZHAO, and Yanqing HAN declare that they have no conflicts of interest.

This article does not contain any studies with human or animal subjects performed by any of the authors.

References

Abidian MR, Daneshvar ED, Egeland BM, et al., 2012. Hybrid conducting polymer—hydrogel conduits for axonal growth and neural tissue engineering. *Adv Healthc Mater*, 1(6):762-767. https://doi.org/10.1002/adhm.201200182

Ahn HS, Hwang JY, Kim SM, et al., 2015. Carbon-nanotube-interfaced glass fiber scaffold for regeneration of transected sciatic nerve. *Acta Biomater*, 13:324-334. https://doi.org/10.1016/j.actbio.2014.11.026

Bhaskar B, Owen R, Bahmaee H, et al., 2018. Composite porous scaffold of PEG/PLA support improved bone matrix deposition *in vitro* compared to PLA-only scaffolds. *J Biomed Mater Res A*, 106(5):1334-1340. https://doi.org/10.1002/jbm.a.36336

Bosi S, Ballerini L, Prato M, 2014. Carbon nanotubes in tissue engineering. *In*: Marcaccio M, Paolucci F (Eds.), Making and Exploiting Fullerenes, Graphene, and Carbon Nanotubes. Springer, Berlin, p.181-204. https://doi.org/10.1007/128_2013_474

Duan B, Gao HM, He M, et al., 2014. Hydrophobic modification on surface of chitin sponges for highly effective separation of oil. *ACS Appl Mater Interfaces*, 6(22):19933-19942. https://doi.org/10.1021/am505414y

Eldesoqi K, Henrich D, El-Kady AM, et al., 2014. Safety evaluation of a bioglass—polylactic acid composite scaffold seeded with progenitor cells in a rat skull critical-size bone defect. *PLoS ONE*, 9(2):e87642. https://doi.org/10.1371/journal.pone.0087642

Fabbro A, Sucapane A, Toma FM, et al., 2013a. Adhesion to carbon nanotube conductive scaffolds forces action-potential appearance in immature rat spinal neurons. *PLoS ONE*, 8(8):e73621. https://doi.org/10.1371/journal.pone.0073621

Fabbro A, Prato M, Ballerini L, 2013b. Carbon nanotubes in neuroregeneration and repair. *Adv Drug Deliv Rev*, 65(15): 2034-2044. https://doi.org/10.1016/j.addr.2013.07.002

Gao JJ, Zhu J, Luo JJ, et al., 2016. Investigation of microporous composite scaffolds fabricated by embedding sacrificial polyethylene glycol microspheres in nanofibrous membrane. *Compos Part A Appl Sci Manuf*, 91:20-29. https://doi.org/10.1016/j.compositesa.2016.09.015

Ghasemi-Mobarakeh L, Prabhakaran MP, Morshed M, et al., 2011. Application of conductive polymers, scaffolds and electrical stimulation for nerve tissue engineering. *J Tissue Eng Regen Med*, 5(4):e17-e35. https://doi.org/10.1002/term.383

Gu XS, Ding F, Williams DF, 2014. Neural tissue engineering options for peripheral nerve regeneration. *Biomaterials*, 35(24):6143-6156. https://doi.org/10.1016/j.biomaterials.2014.04.064

He M, Wang ZG, Cao Y, et al., 2014. Construction of chitin/PVA composite hydrogels with jellyfish gel-like structure and their biocompatibility. *Biomacromolecules*, 15(9):3358-3365. https://doi.org/10.1021/bm500827q

Huang Y, Zhong ZB, Duan B, et al., 2014. Novel fibers fabricated directly from chitin solution and their application as wound dressing. *J Mater Chem B*, 2(22):3427-3432. https://doi.org/10.1039/c4tb00098f

Ifuku S, Saimoto H, 2012. Chitin nanofibers: preparations, modifications, and applications. *Nanoscale*, 4(11):3308-3318. https://doi.org/10.1039/c2nr30383c

Jayakumar R, Prabaharan M, Kumar PTS, et al., 2011. Biomaterials based on chitin and chitosan in wound dressing applications. *Biotechnol Adv*, 29(3):322-337. https://doi.org/10.1016/j.biotechadv.2011.01.005

Ji CD, Annabi N, Hosseinkhani M, et al., 2012. Fabrication of poly-DL-lactide/polyethylene glycol scaffolds using the gas foaming technique. *Acta Biomater*, 8(2):570-578. https://doi.org/10.1016/j.actbio.2011.09.028

Kotturi H, Abuabed A, Zafar H, et al., 2017. Evaluation of polyethylene glycol diacrylate-polycaprolactone scaffolds for tissue engineering applications. *J Funct Biomater*, 8(3):39. https://doi.org/10.3390/jfb8030039

Lau C, Cooney MJ, Atanassov P, 2008. Conductive macroporous composite chitosan-carbon nanotube scaffolds. *Langmuir*, 24(13):7004-7010. https://doi.org/10.1021/la8005597

Liu XF, Miller AL II, Park S, et al., 2016. Covalent crosslinking of graphene oxide and carbon nanotube into hydrogels enhances nerve cell responses. *J Mater Chem B*, 4(43):6930-6941. https://doi.org/10.1039/c6tb01722c

Ma SQ, Chen Z, Qiao F, et al., 2014. Guided bone regeneration with tripolyphosphate cross-linked asymmetric chitosan membrane. *J Dent*, 42(12):1603-1612. https://doi.org/10.1016/j.jdent.2014.08.015

Mattioli-Belmonte M, Vozzi G, Whulanza Y, et al., 2012. Tuning polycaprolactone—carbon nanotube composites for bone tissue engineering scaffolds. *Mater Sci Eng C*, 32(2):152-159. https://doi.org/10.1016/j.msec.2011.10.010

Mauro N, Manfredi A, Ranucci E, et al., 2013. Degradable poly (amidoamine) hydrogels as scaffolds for in vitro culturing of peripheral nervous system cells. *Macromol Biosci*, 13(3):332-347. https://doi.org/10.1002/mabi.201200354

Mehdikhani M, Ghaziof S, 2018. Electrically conductive poly-ε-caprolactone/polyethylene glycol/multi-wall carbon nanotube nanocomposite scaffolds coated with fibrin glue for myocardial tissue engineering. *Appl Phys A*, 124:77. https://doi.org/10.1007/s00339-017-1474-4

Nagarajan S, Belaid H, Pochat-Bohatier C, et al., 2017. Design of boron nitride/gelatin electrospun nanofibers for bone tissue engineering. *ACS Appl Mater Interfaces*, 9(39):33695-33706. https://doi.org/10.1021/acsami.7b13199

Naumenko E, Fakhrullin R, 2019. Halloysite nanoclay/biopolymers composite materials in tissue engineering. *Biotechnol J*, 14(12):1900055. https://doi.org/10.1002/biot.201900055

Nisbet DR, Crompton KE, Horne MK, et al., 2008. Neural tissue engineering of the CNS using hydrogels. *J Biomed Mater Res Part B Appl Biomater*, 87B(1):251-263. https://doi.org/10.1002/jbm.b.31000

Park SY, Choi DS, Jin HJ, et al., 2011. Polarization-controlled differentiation of human neural stem cells using synergistic cues from the patterns of carbon nanotube monolayer coating. *ACS Nano*, 5(6):4704-4711. https://doi.org/10.1021/nn2006128

Posypanova GA, Gayduchenko IA, Moskaleva EY, et al., 2016. Neuronal differentiation of PC12 cells and mouse neural stem cells on carbon nanotube films. *Cell Tissue Biol*, 10(3):194-201. https://doi.org/10.1134/S1990519X16030111

Rad SM, Khorasani MT, Joupari MD, 2016. Preparation of HMWCNT/PLLA nanocomposite scaffolds for application in nerve tissue engineering and evaluation of their physical, mechanical and cellular activity properties. *Polym Adv Technol*, 27(3):325-338. https://doi.org/10.1002/pat.3644

Runge MB, Dadsetan M, Baltrusaitis J, et al., 2010. Development of electrically conductive oligo(polyethylene glycol) fumarate-polypyrrole hydrogels for nerve regeneration. *Biomacromolecules*, 11(11):2845-2853. https://doi.org/10.1021/bm100526a

Şen Ö, Culha M, 2016. Boron nitride nanotubes included thermally cross-linked gelatin—glucose scaffolds show improved properties. *Colloids Surf B Biointerfaces*, 138:41-49. https://doi.org/10.1016/j.colsurfb.2015.11.036

Shitole AA, Giram PS, Raut PW, et al., 2019. Clopidogrel eluting electrospun polyurethane/polyethylene glycol thromboresistant, hemocompatible nanofibrous scaffolds. *J Biomater Appl*, 33(10):1327-1347. https://doi.org/10.1177/0885328219832984

Shokrgozar MA, Mottaghitalab F, Mottaghitalab V, et al., 2011. Fabrication of porous chitosan/poly(vinyl alcohol) reinforced single-walled carbon nanotube nanocomposites for neural tissue engineering. *J Biomed Nanotechnol*, 7(2):276-284. https://doi.org/10.1166/jbn.2011.1284

Srinivasan A, Teo N, Poon KJ, et al., 2021. Comparative craniofacial bone regeneration capacities of mesenchymal stem cells derived from human neural crest stem cells and bone marrow. *ACS Biomater Sci Eng*, 7(1):207-221. https://doi.org/10.1021/acsbiomaterials.0c00878

Stock K, Nolden L, Edenhofer F, et al., 2010. Transcription factor-based modulation of neural stem cell differentiation using direct protein transduction. *Cell Mol Life Sci*, 67(14):2439-2449. https://doi.org/10.1007/s00018-010-0347-1

Suner SS, Demirci S, Yetiskin B, et al., 2019. Cryogel composites based on hyaluronic acid and halloysite nanotubes as scaffold for tissue engineering. *Int J Biol Macromol*, 130:627-635. https://doi.org/10.1016/j.ijbiomac.2019.03.025

Teo AJT, Mishra A, Park I, et al., 2016. Polymeric biomaterials for medical implants and devices. *ACS Biomater Sci Eng*, 2(4):454-472.

https://doi.org/10.1021/acsbiomaterials.5b00429

Türk S, Altınsoy I, Efe GÇ, et al., 2018. 3D porous collagen/functionalized multiwalled carbon nanotube/chitosan/hydroxyapatite composite scaffolds for bone tissue engineering. *Mater Sci Eng C*, 92:757-768. https://doi.org/10.1016/j.msec.2018.07.020

Uto K, Mano SS, Aoyagi T, et al., 2016. Substrate fluidity regulates cell adhesion and morphology on poly (ε-caprolactone)-based materials. *ACS Biomater Sci Eng*, 2(3):446-453. https://doi.org/10.1021/acsbiomaterials.6b00058

van den Broeck L, Piluso S, Soultan AH, et al., 2019. Cytocompatible carbon nanotube reinforced polyethylene glycol composite hydrogels for tissue engineering. *Mater Sci Eng C*, 98:1133-1144. https://doi.org/10.1016/j.msec.2019.01.020

Venkatesan J, Ryu BM, Sudha PN, et al., 2012. Preparation and characterization of chitosan-carbon nanotube scaffolds for bone tissue engineering. *Int J Biol Macromol*, 50(2):393-402. https://doi.org/10.1016/j.ijbiomac.2011.12.032

Wang JY, Sun PP, Bao YM, et al., 2011. Cytotoxicity of single-walled carbon nanotubes on PC12 cells. *Toxicol in Vitro*, 25(1):242-250. https://doi.org/10.1016/j.tiv.2010.11.010

Wu J, Meredith JC, 2014. Assembly of chitin nanofibers into porous biomimetic structures via freeze drying. *ACS Macro Lett*, 3(2):185-190. https://doi.org/10.1021/mz400543f

Wu SQ, Duan B, Zeng XP, et al., 2017. Construction of blood compatible lysine-immobilized chitin/carbon nanotube microspheres and potential applications for blood purified therapy. *J Mater Chem B*, 5(16):2952-2963. https://doi.org/10.1039/c7tb00101k

Xu DF, Fan L, Gao LF, et al., 2016. Micro-nanostructured polyaniline assembled in cellulose matrix via interfacial polymerization for applications in nerve regeneration. *ACS Appl Mate Interfaces*, 8(27):17090-17097. https://doi.org/10.1021/acsami.6b03555

Zhou ZF, Liu XF, Wu W, et al., 2018. Effective nerve cell modulation by electrical stimulation of carbon nanotube embedded conductive polymeric scaffolds. *Biomater Sci*, 6(9):2375-2385. https://doi.org/10.1039/c8bm00553b